Observation of Detonation Initiation by a High-speed Spherical Projectile Using the Diaphragmless Method

Shinichi Maeda, Ryoto Sato, Ken Suzuki, Yoko Seki, and Tetsuro Obara
Graduate School of Science and Engineering, Saitama University
Saitama City, Saitama, Japan

1 Introduction

When a projectile enters a combustible mixture at hypersonic speed, the shock wave formed around the projectile adiabatically compresses the combustible mixture, induces combustion, and the combustion wave is sustained around the projectile. This phenomenon is called shock-induced combustion. Detonation waves can be initiated by the projectile if the reactivity of the mixture is sufficiently high relative to the energy input to the mixture by the projectile. Furthermore, if the speed of the projectile exceeds the Chapman-Jouguet (C-J) detonation velocity, oblique detonation waves are formed, in which the detonation initiated directly by the projectile is sustained around the projectile. These combustion phenomena have been proposed for application to the combustion process of future hypersonic propulsion systems, which are called as shock-induced combustion ramjets [1] and oblique detonation engines [2]. While these applications are the final engineering goal, there have been many fundamental studies focusing on the interesting feature that various combustion modes can be observed despite the very simple configuration of the spherical projectile in free flight in the combustible mixture. Shock-induced combustion with oscillation of the reaction front has attracted attention in the past [3-7], and many studies have been conducted on direct initiation of detonation [8-10] and stabilization of oblique detonation [11-14] by the projectiles. In most of the studies, single-frame or multi-frame visualization of the combustion regimes have been made, but there are few optical observations of the detonation initiation process by the projectile. Although detailed experimental studies [8] conducted on the direct initiation of detonation by the spherical projectile under conditions where the projectile Mach number was lower than the C-J detonation Mach number, detailed information on the initiation process was not available because the detonation initiation was detected only by pressure measurements. In general, in the direct initiation of detonation, the strong blast wave exceeding the C-J detonation Mach number is generated in a combustible mixture using a powerful energy source, and coupling between the shock wave and the reaction front with cellular instability develops as the blast wave decays to the C-J detonation Mach number [15]. On the other hand, it is interesting to see how the detonation occurs when the projectile Mach number (i.e., the shock wave Mach number formed around the projectile) is lower than the C-J detonation Mach number. However, it is difficult to observe the initiation process under such conditions because the initiated detonation propagates quickly overtaking the projectile.

Recently, we attempted to directly observe the phenomena immediately after the projectile entered the reactive mixture by launching the projectile into the combustible mixture filled with the transparent soap

Correspondence to: shinichimaeda@mail.saitama-u.ac.jp

bubble formed in the visualization area [16]. Interesting observations were obtained, including the detonation initiation process by the projectile using this technique. However, it was also found that there were some issues that there was a limit to the size of the soap bubbles that could be generated and that the reactivity of the combustible mixture in the soap bubbles was indicated to decrease over time. Therefore, in this study, we attempted to use the remotely controllable slide valve as the new method that does not use soap bubbles. With this method, we confirmed the validity of our previous results using the soap bubbles, observed the detonation initiation process, and investigated the effect of the argon dilution ratio of the hydrogen/oxygen mixture on the detonation initiation criteria.

2 Experimental apparatus and conditions

Figure 1 shows a schematic of the experimental apparatus. It consisted of the high-speed gas gun, the buffer chamber connected to the gas gun and the observation chamber. The spherical projectile was launched by the gas gun into the combustible mixture, which was filled in the observation chamber. The observation chamber was equipped with a pair of optical windows that allowed to visualize the combustion phenomena around the projectile. The slide valve (steel plate) was located at the left end of the field of view of the optical system. The buffer chamber (upstream of the slide valve) was filled with nitrogen gas, and the observation chamber (downstream of the slide valve) was filled with the combustible mixture. The nitrogen gas and combustible mixture were filled at the same pressure, and the four electromagnets attracted and sealed the slide valve to the surface where the O-ring was installed. The spring in Fig. 1 held the wiring of the electromagnets in place to prevent it from colliding with the free-flight projectile. When the electromagnets were turned off just before the projectile was launched, the slide valve dropped down to open the flight path of the projectile. This allowed the projectile to across the interface between the nitrogen gas and the combustible mixture and enter the field of view of the optical system. The optical system consisted of the high-speed camera (nac Image Technology Inc., ULTRA Cam HS-106E) and schlieren optical system. The high-speed camera recorded with the frame speed of 500,000 fps and the exposure time of 0.3 µs The combustible mixture was $2H_2 + O_2 + 3Ar$ and $2H_2 + O_2 + 7Ar$ mixtures, and the initial pressure was 70 kPa to 105 kPa for the 3Ar cases and 105 kPa to 120 kPa for 7Ar cases. The projectile was the 10 mm diameter sphere and was launched at the Mach number in the range of 3 to 6.5.

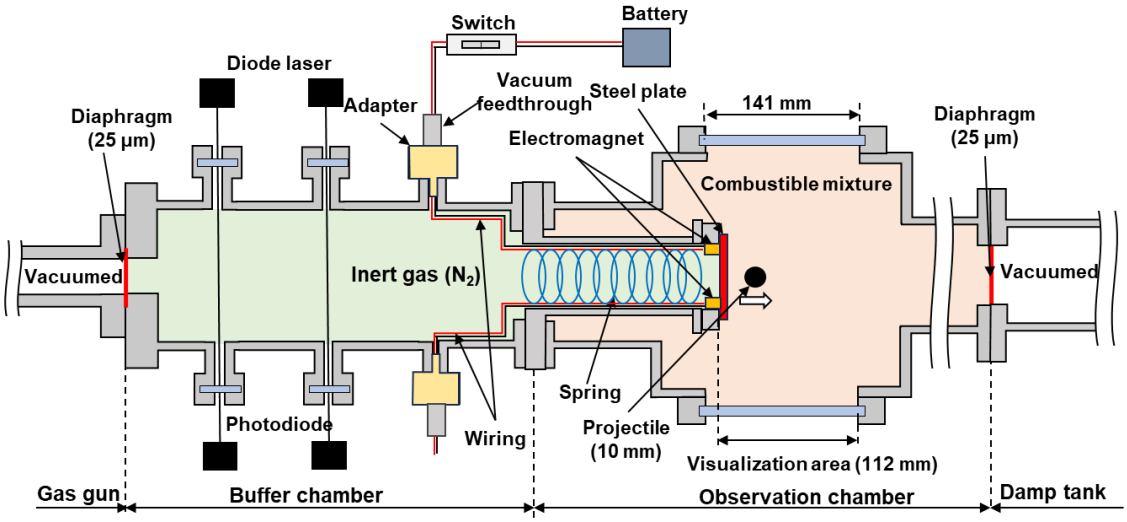

Figure 1: Schematic of experimental setup.

3 Results and discussion

Typical shadowgraph snapshots of the combustion regimes observed in this study are shown in Fig. 2. For clearly showing the combustion regime, each image was processed to eliminate the background noise. Figures 2 (a) and (b) shows the shock-induced combustion, in which the reaction front without and with the oscillational instability, respectively. The oscillational instability with large amplitude is generally known to occur under conditions in the vicinity of the critical condition for detonation initiation. Figure 2 (c) shows the conditions under which the detonation initiation was observed, especially when the projectile Mach number was lower than the C-J detonation Mach number. Figure 2 (d) is another condition in which the detonation was initiated by the projectile, but the projectile Mach number was higher than the C-J detonation Mach number, so the oblique detonation wave was sustained around the projectile. These combustion regimes through (a) to (d) were similar to that observed in our previous study [16] using the soap bubble.

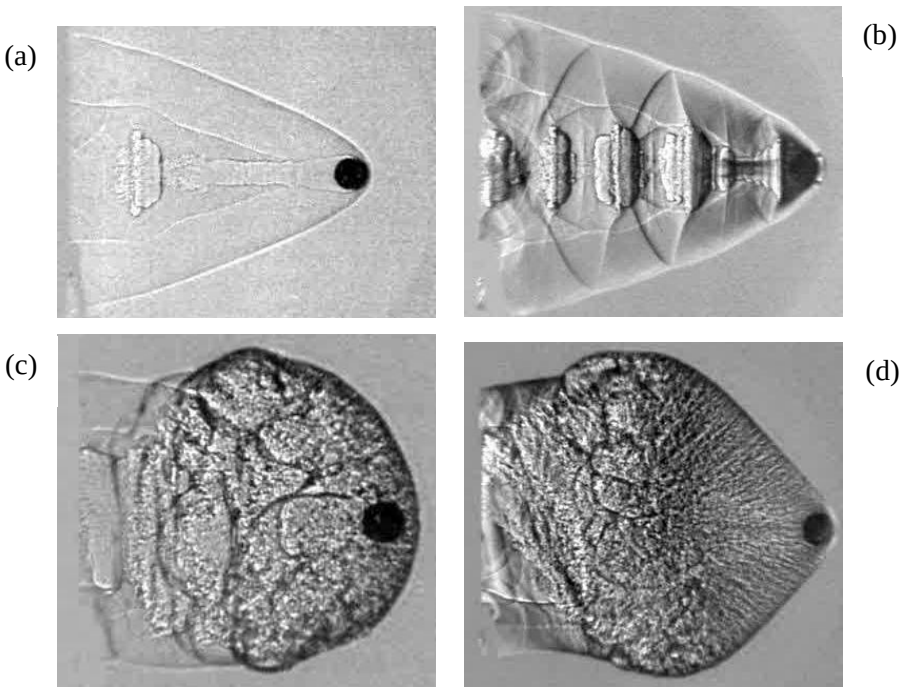

Figure 2: Observed combustion regimes; (a) Shock-induced combustions without combustion instability ($2H_2 + O_2 + 3Ar$, $d / \lambda = 5.0$, $M_p / M_{CJ} = 0.73$), (b) Shock-induced combustions with combustion instability ($2H_2 + O_2 + 7Ar$, $d / \lambda = 7.6$, $M_p / M_{CJ} = 0.72$) (c) Detonation initiation ($2H_2 + O_2 + 3Ar$, $d / \lambda = 6.3$, $M_p / M_{CJ} = 0.92$), (d) Oblique detonation wave ($2H_2 + O_2 + 3Ar$, $d / \lambda = 6.3$, $M_p / M_{CJ} = 1.28$), where M_p: projectile Mach number, M_{CJ}: C-J detonation Mach number, d: projectile diameter, λ: detonation cell width

In this study, the experiments using the slide valve enabled to give the optical observation of the detonation initiation process from the instant when the projectile entered the combustible mixture, and the characteristic initiation process was observed similar to that observed with the soap bubble method [16]. Figures 3 (a) and (b) shows the time sequential pictures of the detonation initiation process in Figs. 2 (c) and (d), respectively. The time of each image is the elapsed time when the projectile entered the combustible mixture. In Fig. 3 (a), the reaction front formed behind the projectile originally showed the characteristic of the large disturbance regime (LDR) [4], in which the large amplitude oscillations of the reaction front occur with the longer period than the ignition delay time behind the shock wave. In the front of projectile, the multiple detonation initiations occurred over time at the positions indicated by DW1 through DW3. The detonation waves generated by these initiations eventually develop around the projectile, and the detonation wave spread into the combustible mixture. The numerical simulation by

Matsuo and Fujii [6] suggested that the detonation can be generated locally in front of the projectile in the LDR. The results of this study indicates that under conditions where the projectile Mach number is lower than the C-J detonation Mach number, these locally initiated detonations can develop into the self-sustained detonation that spreads throughout the combustible mixture.

On the other hand, Fig. 3 (b) shows the time sequential pictures of the development process of oblique detonation in Fig. 2 (d). Since the projectile Mach number was sufficiently higher than the C-J detonation Mach number, the overdriven detonation was initiated directly to the front of the projectile at the instant the projectile entered the combustible mixture. As this overdriven detonation developed outward from the projectile, it lost the support of the projectile body and eventually decayed into the C-J detonation under the influence of expansion wave, forming the oblique detonation. The area of oblique detonation was observed to expand with the propagation of oblique detonation wave shown as red arrows from 14 μs to 40 μs in Fig. 3 (b). This result was very similar to that observed by Maeda et al. [12], when they observed the initiation process immediately after the spherical projectile broke through the thin PET diaphragm and entered the combustible mixture filled in the observation chamber.

Careful observation of the time-series image in Fig. 3 shows that the combustion wave within about 20 mm from the left edge of the image was clearly different from the combustion further downstream, where the projectile passed immediately downstream the interface between the nitrogen gas and combustible mixture. The combustion in the vicinity of the interface was much smoother than the combustion further downstream, as the instability of the reaction front was suppressed. This is considered to be due to the effect of nitrogen gas filled upstream of the slide valve diffusing into the combustible mixture by the time (about 1 to 2 seconds) between the slide valve opening and the launching of the projectile.

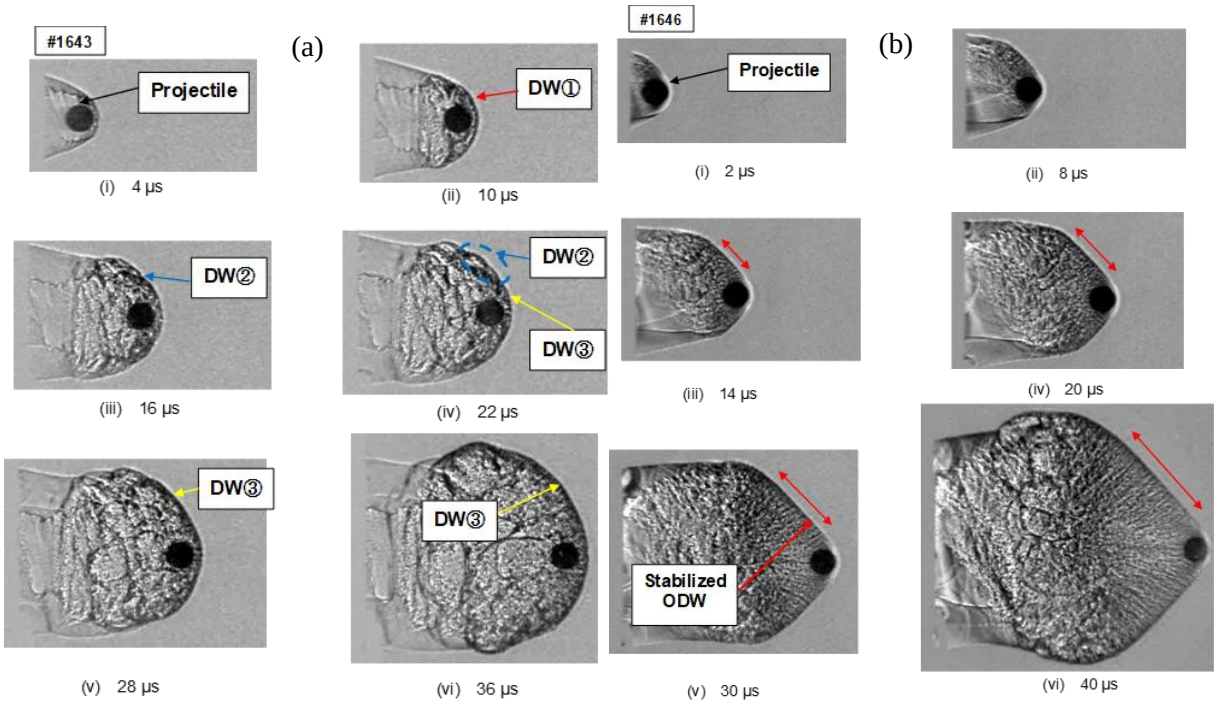

Figure 3: Time sequential shadowgraph pictures of the (a) detonation initiation and (b) oblique detonation regimes in Figs. 2 (c) and (d), respectively.

Then, we discuss the effect of the argon dilution ratio of the hydrogen/oxygen mixture on the detonation initiation criteria. The critical conditions for the detonation initiation [8, 9] and for the stabilization of oblique detonation [11-13] by the spherical projectiles have been expressed by the ratio (d / λ) of projectile diameter, d to detonation cell width, λ. Lee [9] proposed the semi-empirical

expression for the critical condition for detonation initiation as $M_p / M_{CJ} = 5.3\ (\lambda / d)$ and it was carefully validated by the experiments of Higgins and Bruckner [8], where, M_p is the projectile Mach number and M_{CJ} is the C-J detonation Mach number. On the other hand, the variation of critical conditions with different amount of argon dilution was experimentally indicated for the stabilization of oblique detonation wave [11-13] under the condition $M_p > M_{CJ}$, which was around $d / \lambda = 3.5$ and 5.5 for 50 % and 75 % Ar dilution mixture, respectively. Figure 4 shows the classification of the combustion regimes observed in this study with the M_p / M_{CJ} on the horizontal axis and the d / λ on the vertical axis. The solid curve in the figure is the semi-empirical equation by Lee [9] described above. The conditions under which the detonation initiation was observed were consistent with the Lee's equation in the condition around $0.8 < M_p / M_{CJ}$ of $2H_2 + O_2 + 3Ar$ mixture, and the conditions under which the oblique detonation was observed for $M_p > M_{CJ}$ were also approximately consistent with the reported critical condition in both mixtures. The Lee's semi-empirical equation was derived purely from the energetic requirement for detonation initiation. The lack of detonation initiation even for the large d / λ in the region of M_p / M_{CJ} less than 0.8 may be due to the autoignition limit, which was also observed in the experiment of Higgins and Bruckner [8]. On the other hand, the $2H_2 + O_2 + 7Ar$ mixture under the conditon of $M_p < M_{CJ}$ indicated the different results from the 3Ar cases, and the criterion expressed as the d / λ shifted toward less likely to occur the detonation initiation. In the critical tube diameter problem of the detonation re-initiation, the critical condition based on the detonation cell width is known to fail for the mixture with the large amounts of argon dilution, and the critical tube diameter become well above the 13λ [15]. It has been reported that the stabilization limit for the oblique detonation around the spherical projectile was similarly affected by the argon dilution ratio. The results of this study also indicated that even for the direct initiation of the detonation by the spherical projectile under the $M_p < M_{CJ}$ conditions, the large amount of argon dilution increased the initiation criteria based on the cell width.

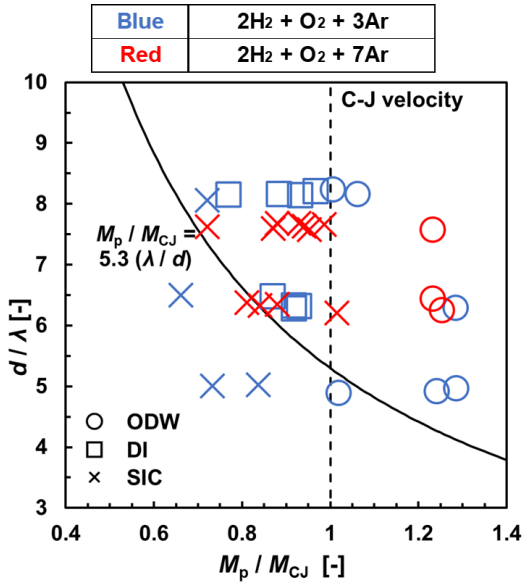

Figure 4: Observed combustion regimes for each condition of M_p / M_{CJ} and d / λ. ODW: oblique detonation wave, DI: detonation initiation, SIC: shock-induced combustion

4 Conclusions

In this study, the spherical projectile was launched at supersonic to hypersonic speed into the combustible using the diaphragmless method consisting of the slide valve driven by the electromagnet. This method allowed to visualize the detailed process of detonation initiation immediately after the projectile entered the combustible mixture, avoiding the effect of diaphragm rupture by the projectile. The detonation initiation process was observed when the projectile Mach number was lower than the

C-J detonation Mach number. It was observed that the multiple localized detonation initiation occurred at the front of the projectile in accordance with the unsteady oscillating combustion, which eventually developed into the detonation wave that spread to the entire combustible mixture, which was similar to that observed in our previous study using the soap bubble method. It was found that the argon dilution ratio affected the criteria for the detonation initiation based on the cell width. As with the critical tube diameter problem and the stabilization conditions for oblique detonation, the higher argon dilution ratios were found to result in the higher critical values.

References

[1] Dudebout, R., Sislian, J.P. and Oppitz, R., Numerical simulation of hypersonic shock-induced combustion ramjets, Journal of Propulsion and Power, Vol.14, No.6 (1998), pp.869-879.

[2] Wolanski, P., Detonative propulsion, Proceedings of the Combustion Institute, Vol.34 (2013), pp.125-158.

[3] McVey, J.B. and Toong, T.Y., Mechanism of instabilities of exothermic hypersonic blunt-body flows, Combustion Science and Technology, Vol.3 (1971), pp.63-76.

[4] Alpert, R.L. and Toong, T.Y., Periodicity in exothermic hypersonic flows about blunt projectiles, Astronautica Acta, Vol.17 (1972), pp.539-560.

[5] Lehr, H.F., Experiments on shock-induced combustion, Astronautica Acta, Vol.17 (1972), pp.589-597.

[6] Matsuo, A. and Fujii, K., Computational study of large-disturbance oscillations in unsteady supersonic combustion around projectiles, AIAA Journal, Vol.33, No.10 (1995), pp.1828-1835.

[7] Matsuo, A. and Fujii, K., Prediction method of unsteady combustion around hypersonic projectile in stoichiometric hydrogen-air, AIAA Journal, Vol.36, No.10 (1998), pp.1834-1841.

[8] Higgins, A.J. and Bruckner, A.P., Experimental investigation of detonation initiation by hypervelocity blunt projectiles., AIAA paper, 96-0342 (1996).

[9] Lee, J.H.S., Initiation of detonation by a hypervelocity projectile, Progress in Astronautics and Aeronautics, Vol.173 (1997), pp.293-310.

[10] Vasiljev, A.A., Initiation of gaseous detonation by a high speed body, Shock Waves, Vol.3, No.4 (1994), pp.321-326.

[11] Kasahara, J., Arai, T., Chiba, S., Takazawa, K., Tanahashi, Y. and Matsuo, A., Criticality for stabilized oblique detonation wave around spherical bodies in acetylene/oxygen/krypton mixtures, Proceedings of the Combustion Institute, Vol.29 (2002), pp.2817-2824.

[12] Maeda, S., Sumiya, S., Kasahara, J. and Matsuo, A., Initiation and sustaining mechanisms of stabilized Oblique Detonation Waves around projectiles, Proceedings of the Combustion Institute, Vol.34 (2013), pp.1973-1980.

[13] Maeda, S., Sumiya, S., Kasahara, J. and Matsuo, A., Scale effect of spherical projectiles for stabilization of oblique detonation waves, Shock Waves, Vol.25, No.2 (2015), pp.141-150.

[14] Kaneshige, M.J. and Shepherd, J.E., Oblique detonation stabilized on a hypervelocity projectile, Symposium (International) on Combustion, Vol.26, No.2 (1996), pp.3015-3022.

[15] Lee, J.H.S., The Detonation Phenomenon. Cambridge University Press, New York (2008)

[16] Maeda, S., Hanyu, N., Hiraoka, Y., Sato, R., Nomura, K. and Obara, T., Visualization of Detonation Initiation by a Spherical Projectile Launched into The Soap Bubble Filled with a Combustible Mixture, 29th ICDERS proceedings (2023)